Rheology of Phase Separation in Anisotropic Melt Polymers

S. L. Wunder* and S. Ramachandran

Textile Fibers Department, E. I. du Pont de Nemours & Co., Inc., Experimental Station, Wilmington, Delaware 19898

C. R. Gochanour and M. Weinberg

Central Research and Development Department, E. I. du Pont de Nemours & Co., Inc., Experimental Station, Wilmington, Delaware 19898. *Received March 4, 1985*

ABSTRACT: The temperature dependence of the steady-shear viscosity of three thermotropic polyesters (3,4′-dihydroxybenzophenone terephthalate, the copolymer of 3,4′-dihydroxybenzophenone and resorcinol in the mole ratio 97.5/2.5 with terephthalic acid, and the copolymer of phenylhydroquinone with terephthalic and isophthalic acids in the mole ratio 80/20) was studied as a function of shear rate by using a capillary rheometer. These systems exhibit biphasic behavior over temperature intervals of approximately 10, 15, and 50 °C, respectively, as determined by polarizing optical microscopy and thermal analysis (DSC). We have demonstrated that the melt structure dramatically effects their rheological behavior. In particular, the apparent melt viscosity reaches a maximum at a temperature that corresponds to the midpoint of the biphasic interval. In the wholly anisotropic and isotropic phases, the melt viscosity decreases with increasing temperature as expected. The absolute value of the viscosity in the isotropic phase is higher than that in the anisotropic phase, even though it occurs at a higher temperature. The power law coefficient, N, in the relationship $\eta \propto (\dot{\gamma})^{N-1}$ shows a minimum in the biphasic interval, indicating that in this region the melts are most non-Newtonian. With increasing shear rate, the absolute value of the viscosity decreases and the viscosity maximum shifts to higher temperatures, indicating that in a shear field the chains persist in their extended state to higher temperatures.

Introduction

Many liquid crystalline main-chain thermotropic polymers are aromatic polyesters which contain flexible or asymmetrically substituted monomers to depress their melting points. Alternatively, this is achieved through copolymerization with flexible aliphatic monomers or with nonlinear aromatic monomers that disrupt crystalline packing. The melts of these systems can be anisotropic, but introduction of increasing amounts of the monomer which decreases chain stiffness or linearity eventually results in polymers that melt to an isotropic state. Anisotropic melt polymers should, with increasing temperature, undergo a transition to an isotropic phase, but frequently this occurs above the polymer's decomposition temperature. However, the factors that cause depression of the melting points also decrease the region of stability of the anisotropic phase, permitting observation of the transition to an isotropic melt.

As in lyotropic liquid crystals, a region of biphasic behavior is expected, wherein anisotropic and isotropic phases coexist. For lyotropic systems, this region occurs for monodisperse polymer and solvent alone, but factors such as polydispersity[1] can broaden the biphasic gap. In the case of thermotropic liquid crystals, the biphasic region results from polydispersity in either molecular weight or composition. While the rheology of isotropic polymer melts has been extensively investigated and there have been a number of papers on the rheology of lyotropic liquid crystalline polymers,[2] very few reports have appeared on the rheology of thermotropic liquid crystals,[3-5] and there have been no studies on the rheology of phase separation in anisotropic melt polymers.

We have undertaken a detailed examination of the rheological properties of three thermotropic melt polymers that exhibit biphasic behavior. These were a copolymer of phenylhydroquinone with terephthalic and isophthalic acids in the mole ratio 80/20, henceforth referred to as PHHQ–T/I (80/20), the homopolymer 3,4′-dihydroxybenzophenone terephthalate (3,4′-DHBP-T), and a copolymer of terephthalic acid with 3,4′-dihydroxybenzophenone and resorcinol in the mole ratio 97.5/2.5, which we will call 3,4′-DHBP/R (97.5/2.5)–T. Their chemical structures are represented in Table I. In order to correlate melt structure with rheological behavior, we characterized the phase transitions by differential scanning calorimetry (DSC) and thermal optical analysis and obtained the temperature dependence of the steady-shear viscosity as a function of shear rate over the same temperature interval. We were particularly interested in exploring possible molecular origins for non-Newtonian behavior in these systems. We studied the behavior of the melt viscosity in the partially melted solid and in the anisotropic, biphasic, and isotropic melts, with the results presented below.

Experimental Methods

The samples of 3,4′-dihydroxybenzophenone terephthalate and the copolymer of terephthalic acid with 3,4′-dihydroxybenzophenone and resorcinol (97.5/2.5) were melt polymerized from terephthalic acid and the diacetates of 3,4′-dihydroxybenzophenone and resorcinol.[6] The copolymer of phenylhydroquinone with terephthalic and isophthalic acid was kindly supplied by J. Zimmerman of E. I. du Pont. It was also melt polymerized by using the diacetate of phenylhydroquinone.[7]

Calorimetric data were obtained with a Du Pont thermal analyzer (Model 1090). The samples were placed in crimped differential scanning calorimetry (DSC) pans and heated at rates of 20 °C/min. A constant flow of dry nitrogen was maintained throughout the runs.

Thermal optical analysis was carried out by using a Leitz polarizing microscope at 320× magnification equipped with a hot stage usable to 400 °C. The samples were melt pressed between two glass cover slips just above their melting points to thicknesses of approximately 5 μm; thicker samples were opaque. The polarization characteristics of the transmitted light were obtained by using the standard crossed-polarizer geometry; only anisotropic materials transmit light in this configuration. A red 1 plate was used to highlight the presence of isotropic material. The sample chamber was continuously purged with nitrogen to prevent sample degradation. A programmable heater was used to heat the samples at 18 °C/min to match the calorimetry scan rate, and the transmitted light intensity was monitored electronically and recorded on a strip chart recorder. A duplicate run under identical

* Address correspondence to Department of Chemistry (016–00), Temple University, Philadelphia, PA 19122.

0024-9297/86/2219-1696$01.50/0

Table I
Chemical Structures of Thermotropic Polyesters

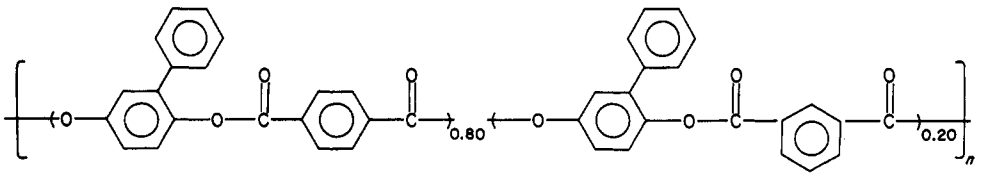

PHHQ-T/I (80/20)

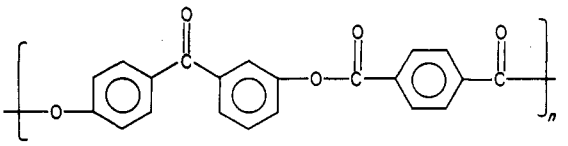

3,4'-DHBP-T

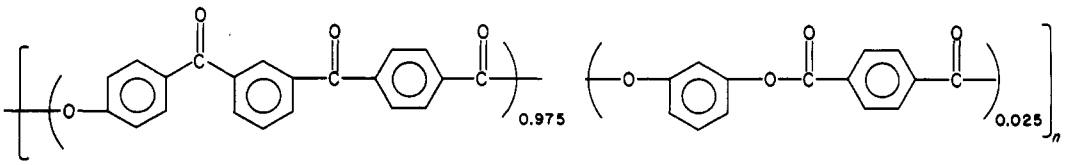

3,4'-DHBP/R (97.5/2.5)-T

Table II
Calorimetric and Optical Transition Temperatures and Molecular Weight Data

	η_{inh}[a]	M_w (GPC) × 10^{-3}	T_g,[b] °C	T_m,[c] °C	T_{AI},[d] °C	T_{flow},[e] °C	T_{min},[f] °C	T_B,[g] °C	T_I,[h] °C
PHHQ–T/I (80/20)	1.2	22.0	144.7	302.0		301	361	380	
3,4'-DHBP-T	1.28	31.6	108.0	282.3	365.2	285	358	365	369
3,4'-DHBP/R(97.5/2.5)–T	1.0	30.0	104.5	276.3	358.9	267	343	354	360

[a] Inherent viscosity, PFP, at 45 °C. [b] T_g = glass transition temperature. [c] T_m = melting temperature, peak position. [d] T_{AI} = anisotropic/isotropic transition temperature, peak position. [e] T_{flow} = temperature at which flow is observed with optical microscope (arrow 1 in Figure 2). [f] T_{min} = temperature in the melt at which minimum in thermal optical plot occurs (arrow 2 in Figure 2). [g] T_B = temperature at which isotropic domains first observed in optical microscope (arrow 3 in Figure 2). [h] T_I = temperature at which melt is completely isotropic as viewed in optical microscope (arrow 4 in Figure 2).

conditions was made while the samples were visually monitored in order to determine their melt texture and morphology.

Intrinsic viscosity data for the polymers were measured in pentafluorophenol at 45 °C. Gel permeation chromatographs of the samples in the solvent pentafluorophenol/hexafluoroisopropyl alcohol (1/40 v/v) with hexafluoroisopropyl alcohol as the carrier fluid were obtained on a Waters 150C instrument using a Du Pont 60s/100s bimodal column set. Poly(ethylene terephthalate) of molecular weight 4×10^4 was used as the calibrant.

The apparent viscosity of the polymers was measured over a shear rate range of approximately 70–14 000 s^{-1} by using an Instron Model 3211 constant-velocity capillary rheometer. The wall shear rate was obtained from $4Q/\pi R^3$, where Q is the flow rate and R is the capillary diameter of die; no correction factors were employed. Proper operation of the rheometer was checked by comparison with measurements on polyethylene (Alathon 7052, a registered trademark of E. I. du Pont & Co., Inc.) for which standard rheological data exist. The rheometer was modified to eliminate piston friction and to increase the operating temperature range to 400 °C. This was accomplished by replacing the seals of Teflon TFE fluorocarbon resin (a registered trademark of E. I. du Pont & Co., Inc.) for the capillary by copper seals and eliminating the O-rings of Teflon fluorocarbon resin on the sliding piston. The leakage of the polymer past the piston was prevented by selecting piston dimensions such that the clearance between the piston and wall of the barrel was less than 0.001 in. Two capillary sizes were used in the experiments, one with a length-to-diameter ratio of 68 (L = 2.00 in., D = 0.0293 in.) and the other with a L/D = 40 (L = 0.8 in., D = 0.02 in.). The larger L/D capillary was used in an attempt to minimize entrance and exit pressure drop effects. However, the data for both capillary sizes were found to overlap. Temperatures quoted were measured with thermocouples mounted in the rheometer barrel and are accurate to about ±5 °C. Measurements of temperature at three points along the rheometer barrel had a variation of less than ±2 °C. To minimize polymer degradation, the rheometer barrel was purged with nitrogen, set about 20 °C below the temperature at which the first measurement was to be obtained, and then loaded with polymer flake under a nitrogen blanket. The samples were always dried for at least 24 h in a nitrogen-purged vacuum oven. The barrel temperature was raised to the temperature at which data were to be taken and allowed to equilibrate for about 5 min. Data points were taken both at increasing and decreasing shear rates to avoid systematic error due to thermal degradation. The absence of systematic variation in the ascending and descending runs is evidence against significant error due to thermal degradation. We also checked inherent viscosities and GPC at the end of the runs, and these did not change within the experimental accuracy of our measurements. Apparent melt viscosities were calculated from standard formulas; no corrections to the data were made.

Results and Discussion

Inherent viscosities and GPC weight-average molecular weights for the samples are listed in Table II. The latter are not true molecular weights because the calibrant was a more flexible polymer (poly(ethylene terephthalate)); the molecular weights reported are thus expected to be too high. The DSC traces for the three polymers, PHHQ–T/I (80/20), 3,4'-DHBP-T, and 3,4'-DHBP/R (97.5/2.5)–T, are shown in parts a, b, and c of Figure 1, respectively, and the transition points are summarized in Table II. Peak positions for the melting temperatures (T_m(max)) are reported, but complete melting is not attained until the endotherm reaches its base-line value. This occurs at 20 °C above T_m(max) for PHHQ–T/I (80/20) and 3,4'-DHBP-T and at 10 °C above T_m(max) for 3,4'-DHBP/R (97.5/2.5)–T. For the latter two polymers, there is a large

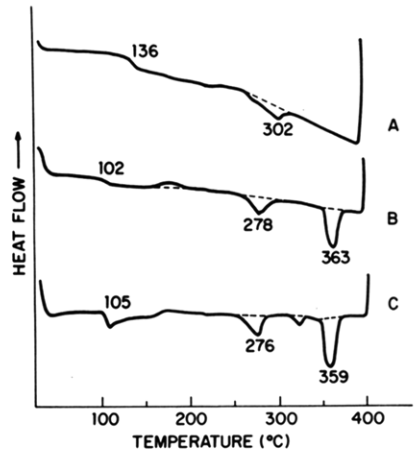

Figure 1. DSC scans of (a) PHHQ–T/I (80/20), (b) 3,4′-DHBP-T, and (c) 3,4′-DHBP/R (97.5/2.5)–T at heating rate of 20 °C/min.

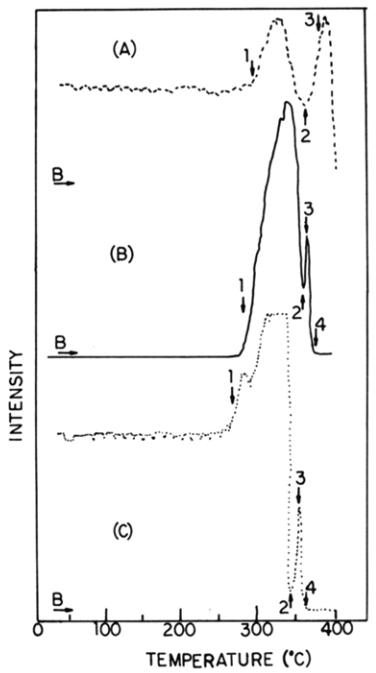

Figure 2. Intensity vs. temperature plots of (a) PHHQ–T/I (80/20), (b) DHBP-T, and (c) 3,4′-DHBP/R (97.5/2.5)–T obtained at a heating rate of 18 °C/min. Arrow 1 indicates flow temperature; 2, temperature at which anisotropic melt darkens; 3, temperature at which isotropic phase first appears; and 4, temperature at which melt becomes completely isotropic. B is the background intensity level.

endothermic peak associated with the anisotropic to isotropic transition (T_{AI}); this assignment is confirmed by optical microscopy as discussed below. In addition, both polymers sometimes exhibited a transition between T_m and T_{AI} (shown only in Figure 1b) which depended on thermal history. It did not occur in the samples we used for the rheology studies. By contrast, no endothermic peaks were observed above T_m(max) for PHHQ–T/I (80/20). As discussed in more detail elsewhere,[8] this is due to the small enthalpy of the nematic/isotropic transition together with its increased breadth. Phase transition points for this polymer were determined by optical microscopy.

Intensity vs. temperature plots for PHHQ–T/I (80/20), 3,4′-DHBP-T, and 3,4′-DHBP/R (97.5/2.5)–T are presented in Figure 2, parts a, b, and c, respectively. Because the light throughput depends on both the sample thickness, which is not fixed, as well as the polymer's anisotropy,

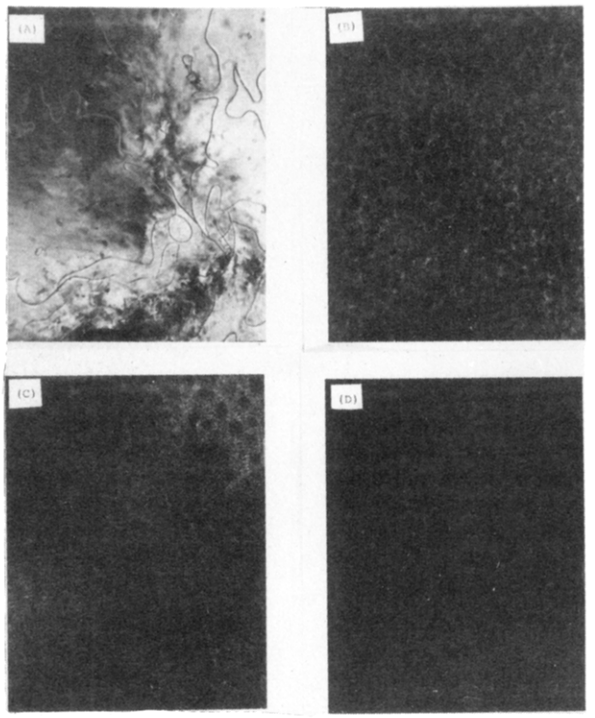

Figure 3. Optical microscope photographs, taken with crossed polarizers and red 1 plate at 320× magnification, of 3,4′-DHBP-T at four temperatures in the melt: (a) 324 °C anisotropic melt; (b) 353 °C biphasic melt, anisotropic phase continuous; (c) 360 °C biphasic melt, isotropic phase continuous; (d) 366 °C isotropic melt.

these plots are only qualitative. Nevertheless, it can be seen that all three polymers exhibit the same pattern of behavior. First, there is a large increase in light throughput at the flow temperature, indicated by arrow 1 in Figure 2. This is followed by a decrease and then an increase in intensity, with the minimum indicated by arrow 2. Finally the intensity drops off again.

The morphological changes associated with the intensity plots were observed visually, and representative photographs are presented in Figures 3 and 4 for 3,4′-DHBP and PHHQ-T/I (80/20), respectively. The major difference between 3,4′-DHBP-T, 3,4′-DHBP/R (97.5/2.5)–T, and PHHQ–T/I (80/20) is in the breadth of the biphasic temperature intervals, which are approximately 10, 15, and 50 °C, respectively, as estimated from the optical measurements. The broadness of the biphasic interval for the latter polymer enabled a more detailed study of the temperature dependence of the melt structure than was possible for the former two. The solid phases of all three polymers (not shown) were birefringent, and their melts exhibited the texture of nematic liquid crystals. This is shown in Figure 3a for 3,4′-DHBP-T. As the temperature was increased, phase separation of isotropic domains, shown in Figure 4a for PHHQ–T/I (80/20), occurred. Arrow 3 of Figure 2 indicates the temperatures at which the isotropic phase was first observed for the polymers. The domains stabilized in size after approximately 5 min (Figure 4b) and grew with increasing temperature (Figures 4c–e and 3b) until phase inversion occurred (Figures 4f and 3c). That is, the continuous phase changed from anisotropic to isotropic. We also observed melt morphologies (Figure 4g) where neither phase was continuous. The complete conversion to a wholly isotropic melt, indicated by arrow 4 in Figure 2, is shown in Figure 3d for 3,4′-DHBP-T.

In the case of 3,4′-DHBP-T and 3,4′-DHBP/R (97.5/2.5)–T the transition temperatures determined calori-

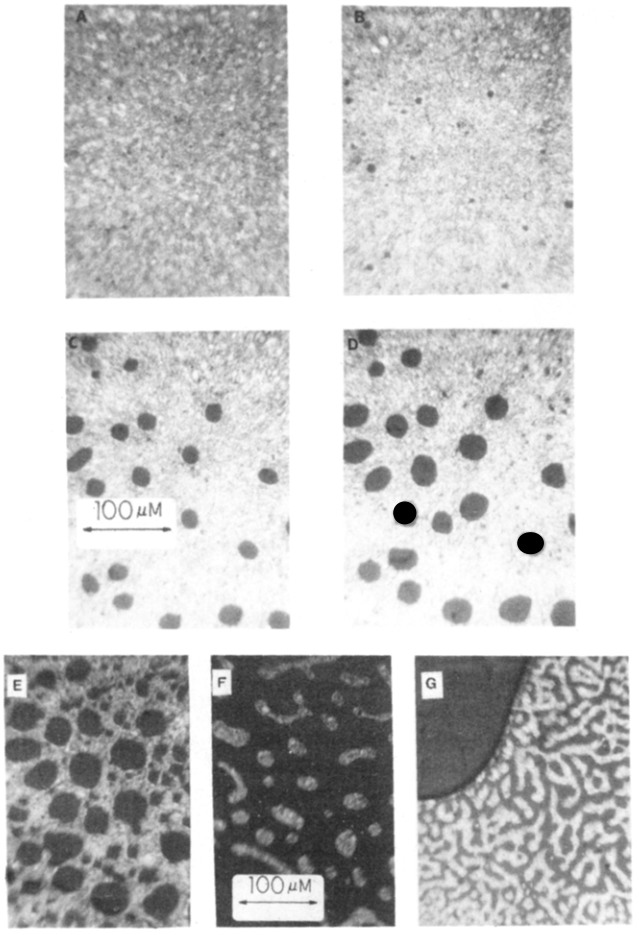

Figure 4. Optical microscope photographs, taken with crossed polarizers and red 1 plate at 320× magnification, of PHHQ–T/I (80/20) in the melt: (a) T = 316 °C, phase separation just beginning; (b) T = 316 °C, 5–10 min later; (c) T = 350 °C, biphasic, anisotropic phase continuous; (d) T = 350 °C, 5–10 min later; (e) T = 362 °C, biphasic, anisotropic phase continuous; (f) T = 362 °C, 5–10 min later; (g) sample cooled to room temperature and reheated to T = 345 °C, both anisotropic and isotropic phases continuous.

metrically and optically are in good agreement, as can be seen by a comparison of the data of Table II. For semicrystalline polymers such as these, one expects the onset of flow to correspond to the melting temperature of the crystals, as we observe. The peak temperature of the anisotropic/isotropic transition (T_{AI}) occurs somewhere between the temperature at which phase separation of isotropic domains is observed and that at which there is a complete conversion to a wholly isotropic state.

In the case of PHHQ–T/I (80/20), there is also good agreement between the calorimetric T_m(max) and the flow temperature, but since we do not observe T_{AI} in the DSC runs, we relied solely on transition temperatures obtained from the optical measurements. The particular PHHQ–T/I (80/20) sample we used for the rheological studies was of higher molecular weight than that used to obtain the photographs of Figure 4. We photographed the lower molecular weight sample to show the range of melt structures in this polymer, but the actual transition temperatures for the sample used in the rheological experiments are presented in Table II and Figure 2. It should be noted that the complete transition to an isotropic state was not complete by 400 °C, the temperature limit of both the optical and rheological equipment.

We do not at present have a definitive explanation of the origin of the darkening and brightening, i.e., arrow 2

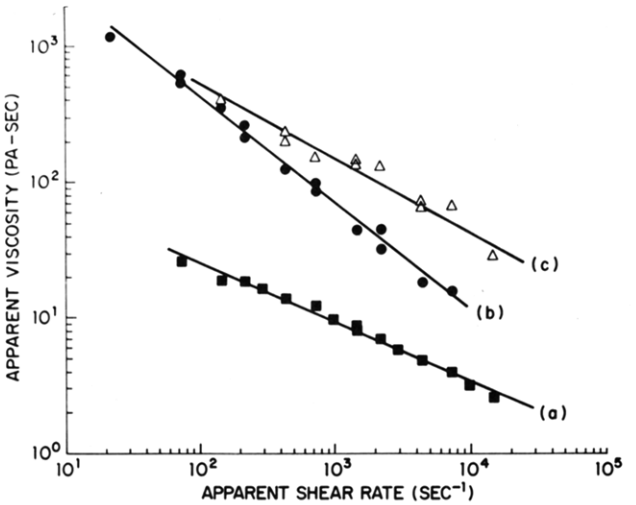

Figure 5. Apparent melt viscosity vs. shear rate for 3,4′-DHBP/R (97.5/2.5)–T at (a) T = 320 °C, anisotropic melt, (b) T = 360 °C, biphasic melt, and (c) T = 400 °C, isotropic melt.

in Figure 2, of the nematic melt before the onset of isotropic phase separation. The magnification of the microscope (320×) permits a resolution of approximately 2 μm, so phase separation of smaller domains at lower temperatures is possible and would be detected electronically (the appearance of isotropic domains are expected to decrease polarized-light throughput) but not observed visually. We noted in another study on these systems that the presence of isotropic domains with dimensions less than 2 μm could be observed by transmission electron microscopy (TEM) when the samples were rapidly quenched from the melt.[8] However, this would not account for the subsequent rise in light throughput that we observe, so the details of the molecular reorganization process in this temperature region are uncertain.

The temperature dependence of the steady-shear viscosity for 3,4′-DHBP–T, 3,4′-DHBP/R (97.5/2.5)–T, and PHHQ–T/I (80/20) was examined as a function of shear rate from just above the respective melting points of the polymers to 400 °C. This range covers the nematic, biphasic, and isotropic regimes and in addition the region between T_m(max) and the temperature of the end of the transition endotherm (from DSC). This was done to simulate the effect of unmelted crystallities in order to observe their effect on the rheological behavior. Typical flow curves of apparent melt viscosity vs. shear rate are shown in Figure 5 for 3,4′-DHBP/R (97.5/2.5)–T in these three phases. The viscosity decreases with increasing shear rate in a power law manner. The power law exponent, N, in the relationship $\eta \propto \dot{\gamma}^{N-1}$ was obtained from linear least-squares fits to all the data at a given temperature. Although slight curvature was observed at low shear rates, we did not restrict the fit to the high shear rate range. The results for all three polymers are presented in Table III and plotted in Figure 6. The power law coefficients show a minimum ($N \simeq 0.2$) in the region where biphasic melts are observed, indicating that the melts become more non-Newtonian over the biphasic interval. Multiphase flow in phase-separated blends[9] is known to produce non-Newtonian behavior in these systems. Non-Newtonian behavior is also observed in both the isotropic and anisotropic melts of these systems at shear rates where polymers such as poly(ethylene terephthalate) (PET) exhibit Newtonian flow (i.e., N = 1); non-Newtonian behavior in PET is usually observed only at shear rates greater than about 1000 s^{-1}. Previous work has demonstrated that as increasing mole fractions of p-hydroxybenzoic acid (PHB)

Table III
Power Law Exponent, N, from $\eta \propto \dot{\gamma}^{N-1}$

	temp, °C	structure	N
PHHQ-T/I (80/20)	310	partially melted solid	0.20
	320	partially melted solid	0.41
	335	anisotropic melt	0.53
	345	anisotropic melt	0.52
	355	anisotropic melt	0.52
	365	anisotropic melt	0.52
	375	biphasic melt	0.46
	385	biphasic melt	0.26
3,4′-DHBP-T	355	anisotropic melt	0.55
	365	biphasic melt	0.22
	375	isotropic melt	0.43
3,4′-DHBP/R (97.5/2.5)-T	270	partially melted solid	0.17
	280	partially melted solid	0.29
	290	partially melted solid	0.34
	300	anisotropic melt	0.48
	320	anisotropic melt	0.58
	325	anisotropic melt	0.55
	340	anisotropic melt	0.50
	360	biphasic melt	0.21
	380	biphasic melt	0.30
	400	isotropic melt	0.51

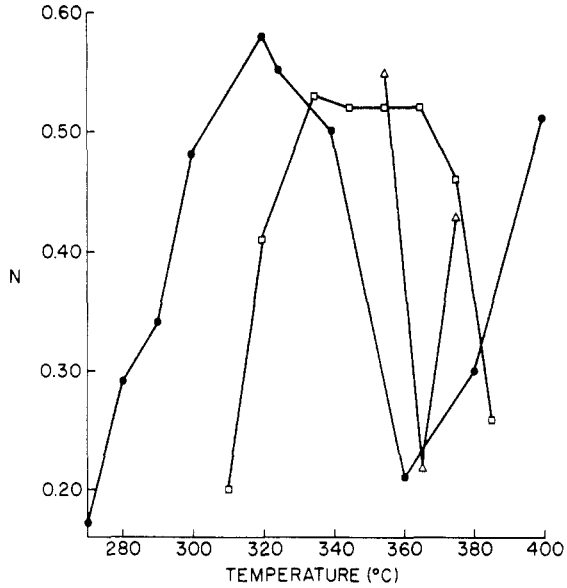

Figure 6. Power law exponent, N, from $\eta \propto \dot{\gamma}^{N-1}$ (where $\dot{\gamma}$ is the shear rate and η is the apparent melt viscosity) for (□) PHHQ-T/I (80/20), (△) 3,4′-DHBP-T, and (●) 3,4′-DHPB/R (97.5/2.5)-T.

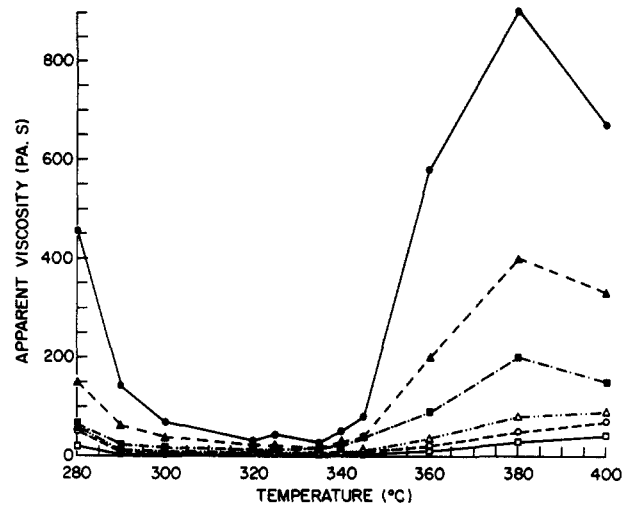

Figure 7. Apparent melt viscosity vs. temperature for 3,4′-DHBP/R (97.5/2.5)-T at the shear rates (s^{-1}) (●) 70, (▲) 235, (■) 706.9, (△) 2356, (○) 4713, and (□) 10 000. Capillary length and diameter were 2.00 in. and 0.0293 in., respectively, L/D = 68.

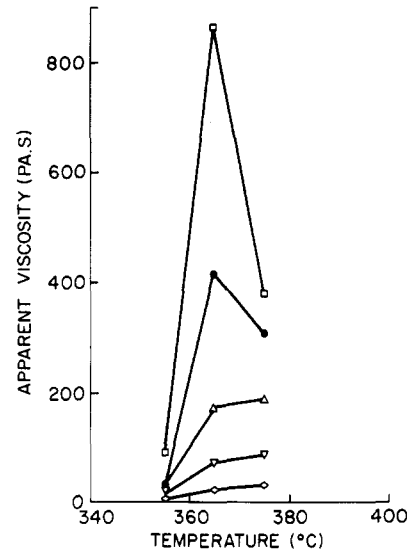

Figure 8. Apparent melt viscosity vs. temperature for 3,4′-DHBP-T at the shear rates (s^{-1}) (□) 70.69, (●) 235.6, (△) 706.9, (▽) 2356, and (◇) 7069. Capillary length and diameter were 0.8 in. and 0.02 in., respectively; L/D = 40.0.

are copolymerized with poly(ethylene terephthalate), the polymers become more shear sensitive at lower shear rates; this parallels the development of liquid crystallinity with increasing PHB content.[11] Similarly, the shear rate dependence of anisotropic poly(phenylhydroquinone terephthalate) begins to exhibit non-Newtonian behavior at lower shear rates than isotropic poly(phenylhydroquinone isophthalate).[12] An interesting feature of our data is that the power law coefficients in the nematic and isotropic phases for the polymers we studied are very nearly equal, with $N \simeq 0.5$. This may be a manifestation of the long relaxation times that have been shown to exist in stiff chain polymers.[2,4,10]

The data we obtained very close to the peak melting points of the polymer [$T_m(\max) \leq T \leq T_m(\max) + 20$ °C], that is, at temperatures where complete melting of all the crystallites had not been achieved, were very non-Newtonian. Values of N between 0.1 and 0.2, indicative of solidlike flow, were observed. Thus it is important to recognize that care must be taken when one extracts molecular information from rheological measurements. Here we see that two separate phenomena, unmelted crystallites and biphasic melt structure, can give rise to the same value of N. In order to correctly attribute molecular origins to particular values of N, it is necessary to have supplemental data from independent experiments. For instance, the existence of unmelted crystalline regions was shown to occur in ultrahigh molecular weight polyethylene by using *Raman* spectroscopy.[13] However, it is very difficult to obtain this type of information for the very high melting thermotropic melt polyesters, which have lower percent crystallinities at room temperature than polyethylene and for which fluorescence is a severe problem (in the Raman experiments).

The most dramatic feature of the flow curves in Figure 5 is the temperature dependence of the absolute magnitude of the apparent viscosity, as has been observed previously by Wissburn and Griffin for another thermotropic polyester.[3] This can be seen most effectively by plotting the temperature dependence of the apparent viscosity at constant-shear rate. The data for several shear rates, ranging from about 70 to 10 000 s^{-1}, are shown in Figures

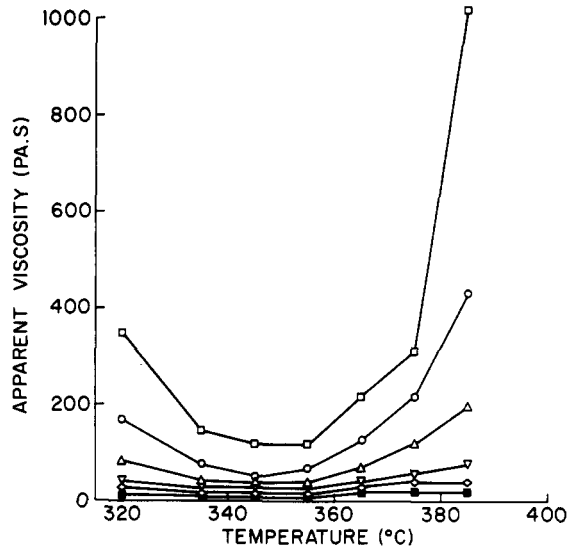

Figure 9. Apparent melt viscosity vs. temperature for PHHQ–T/I (80/20) at the shear rates (s^{-1}) (□) 70.7, (○) 235.6, (△) 706.7, (▽) 2356, (◇) 4713, and (■) 14140. Capillary length and diameter were 0.8 in. and 0.02 in., respectively: L/D = 40.0.

7–9 for 3,4′-DHBP/R (97.5/2.5)–T, 3,4′-DHBP-T, and PHHQ–T/I (80/20), respectively. For some temperatures the data did not quite cover the entire range of shear rates. In these cases, we obtained data points at the highest and lowest shear rates and at fewer intermediate shear rates. For the other shear rates we used extrapolated values from the least-squares fits of the data, which had correlation coefficients of better than 0.97.

At low shear rates the temperature dependence of the apparent viscosity agrees well with what one expects from the phase transitions (at zero shear rate) observed calorimetrically and optically. In regions where the melts are anisotropic, the viscosity decreases with increasing temperature. An Arrhenius temperature dependence (i.e., exponential), characterized by an energy of activation for viscous flow, is expected for single-phase polymer melts, but we made no attempt to fit our limited data points to a particular functional form. The melt viscosity starts to increase at a temperature that corresponds to the point at which the anisotropic melt was observed to darken in the polarizing optical microscope (T_{min} in Table II and arrow 2 in Figure 2). This is below the temperature at which isotropic domains are first observed visually. One possible explanation for this is that the melt viscosity is sensitive to the onset of phase separation of domains smaller than 2 μm. Alternatively, for small-molecule liquid crystals, it is known that the order parameter drops considerably with increasing temperature.[14] The decrease in order parameter as the clearing point is approached has recently been observed for a thermotropic liquid crystalline backbone copolyester by FTIR polarization techniques.[15] Thus the increase in viscosity that we observe 20 °C below the onset of macroscopic phase separation may reflect a decrease in the order parameter over this temperature range.

The maximum in the melt viscosity at low shear rates occurs at a temperature that corresponds well to T_{AI}(max) observed calorimetrically for 3,4′-DHBP-T but at a higher temperature than T_{AI}(max) for 3,4′-DHBP/R (97.5/2.5)–T. Several factors could contribute to this discrepancy. We used 20 °C temperature increments in obtaining the melt rheology data for 3,4′-DHBP/R (97.5/2.5)–T, and better temperature resolution would perhaps improve the agreement with the calorimetric data. Alternatively, the larger number of data points (i.e., temperatures) measured for 3,4′-DHBP/R (97.5/2.5)–T than for 3,4′-DHBP-T necessitated longer total residence times for the polymer in the capillary rheometer. This could result in post-polymerization and thus higher molecular weights which would raise the transition temperatures of the sample.[8] The theoretical work of Matheson[16] on viscosity maxima in lyotropic liquid crystalline systems suggests that the location of the viscosity maximum is dependent on factors such as the shape and morphology of the domains and cannot be predicted precisely without several simplifying assumptions. Thus there is no a priori reason to expect the viscosity maximum to correspond to T_m(max). In the case of PHHQ–T/I (80/20), the maximum melt viscosity was not reached. We expect it to occur somewhere between the temperature of the onset of the biphasic region and the temperature at which the melt is wholly isotropic. This latter phase was not attained in the PHHQ–T/I (80/20) sample we studied. With increased temperature, the melts of 3,4′-DHBP/R (97.5/2.5)–T and 3,4′-DHBP-T became completely isotropic and the apparent viscosity decreased as expected.

The melt viscosity of these polymers is thus well explained in terms of melt structure and reflects the observed phase-separation behavior. There is good agreement between transition points observed calorimetrically, optically, and from melt viscosity, especially in view of the experimental and theoretical uncertainties. A further observation can be made concerning the shapes of the curves in Figures 7–9 at low shear rates. The apparent breadth of the viscosity–temperature plots in the region of biphasic behavior increases in the order PHHQ–T/I (80/20) > 3,4′-DHBP/R (97.5/2.5)–T > 3,4′-DHBP-T. It is shown elsewhere[8] that fractionation by molecular weight and composition results in broadening of the biphasic gap in thermotropic liquid crystalline systems. It is interesting to note here that the rheological behavior is also sensitive to these factors.

The viscosity changes we have reported as a function of temperature have been observed as a function of concentration in lyotropic liquid crystals such as the anisotropic solutions of aromatic polyamides[17] and also as a function of composition for several copolyesters. Melt viscosities of poly(ethylene terephthalate) decrease with increasing mole percent of *p*-hydroxybenzoic acid (PHBA), as this more rigid unit induces liquid crystalline behavior.[11] Similarly, catastrophic decreases of viscosity of between one and three decades in magnitude are observed once a critical terephthalic to isophthalic acid mole ratio is exceeded in the systems phenylhydroquinone–terephthalic/isophthalic acid[8,12] and chlorohydroquinone–4,4-oxydibenzoic acid/terephthalic acid/isophthalic acid;[18] this decrease is also attributable to the formation of an anisotropic melt phase. Previous work in this laboratory[19] using optical microscopy indicated a correlation of biphasic behavior with melt viscosity in methylhydroquinone–terephthalic acid/isophthalic acid compositions.[20]

With increasing shear rate, the maximum viscosity both decreases in absolute value and shifts to higher temperature. At intermediate shear rates, curves with plateau-like shapes are observed. Presumably the viscosity would decrease again at higher temperatures. At the highest shear rates, the viscosity increases monotonically with temperature. The variation in the viscosity maximum with shear rate can be most easily explained as a reflection of the orientation produced with increasing shear. Thus in addition to the thermodynamic order present in the melts, there is a contribution from shear. The clearing point is shifted to increasing temperature with increasing shear

rate. In fact, it is possible that the discrepancy observed between T_m(max) and the viscosity maximum in 3,4′-DHBP/R (97.5/2.5)–T results from shear rate effects. Extrapolation to shear rates of less than 10 s^{-1} might be necessary to approximate the "zero shear" behavior of the static measurements. The generation of flow-induced isotropic-to-anisotropic transitions has been predicted theoretically[21] and observed in solutions of rodlike molecules.[22] In these experiments, shear lowered the critical concentration at which the isotropic-to-nematic transition occurred, but only slightly. A more pronounced shear rate dependence was observed for semirigid polymers, where there was a significant reduction in the concentration of the isotropic to nematic transition.[23] In this case, flow fields could increase the persistence length of the polymers.

The decrease in viscosity and increase of the nematic/isotropic transition temperature at high shear rates is important from a practical viewpoint. When a polyester is melt spun, the shear rate through the capillaries is about 1000 s^{-1}, and when the polymer is injection molded, the shear rate is about 10000 s^{-1}. Thus, at least in the systems we have studied, the biphasic nature of the quiescent melts is not expected to affect the processing of the polymers under normal operating conditions.

Conclusions

The rheology of three thermotropic polyesters was shown to correlate well with the behavior expected on the basis of the phase transitions in these systems. In addition to the observation that the melt viscosity was higher in the isotropic compared with the anisotropic phase, despite its higher temperature, we also demonstrated that a maximum in the melt viscosity occurred in the biphasic temperature interval. In this region, the power law coefficient, N, in the relationship $\eta \propto (\dot{\gamma})^{N-1}$ was a minimum, indicating the very non-Newtonian behavior of the melts. However, we also measured low values of N at temperatures where the polymers were only partially melted, so one must be careful in ascribing molecular origins to rheological behavior without additional experimental information. With increasing shear rate, we observed that the viscosity maximum decreased in absolute value and shifted to higher temperature, indicating that a shear field affects the nematic-to-isotropic transition temperature. We found that the breadth of biphasic interval influenced the shape of the flow curves. This work complements similar and more extensive studies of lyotropic liquid crystals.

Acknowledgment. We express our appreciation to Drs. J. Zimmerman and J. Bloom for providing polymer samples. In addition we thank P. Wilson and R. Dwyer for assistance in obtaining the rheological measurements, R. Twaddell for the calorimetric data, and R. Hempton for the optical tests.

References and Notes

(1) A review and comprehensive list of references can be found in: Flory, P. J. "Molecular Theory of Liquid Crystals" in *Liquid Crystal Polymers*; Gordon, M., Ed.; Springer-Verlag, Berlin, 1984; Vol I.
(2) For recent reviews, see: Baird, D. G. "Rheology of Polymers with Liquid Crystalline Order" in *Liquid Crystalline Order in Polymers*; Blumstein, A., Ed.; Academic: London, 1978, p 237. Wissburn, K. F. *J. Rheol.* **1981**, *25*, 619.
(3) Wissburn, K. F.; Griffin, A. C. *J. Polym. Sci. Polym. Phys. Ed.* **1982**, *20*, 1835.
(4) Wissburn, K. F. *Br. Polym. J.* **1980**, *12*(4), 163.
(5) Cogswell, F. N. *Br. Polym. J.* **1980**, *12*(4), 170.
(6) Irwin, R. S. (Du Pont) U.S. Patent 4 245 082.
(7) Payet, C. R. (Du Pont) U.S. Patent 4 159 365, 1979.
(8) Wunder, S. L., to be published. Zimmerman, J., private communication.
(9) Holden, G.; Bishop, E. T.; Legge, N. R. *J. Polym. Sci., Part C* **1969**, *26*, 37.
(10) Jackson, W. J., Jr. *Br. Polym. J.* **1980**, *12*(4), 154.
(11) Jackson, W. J., Jr.; Kuhfuss, H. F. *J. Polym. Sci., Polym. Chem. Ed.* **1976**, *14*, 2043.
(12) Jackson, W. J., Jr. "Liquid Crystal Polymers: VI. Liquid Crystalline Polyesters of Substituted Hydroquinones" in *Contemporary Topics in Polymer Science*; Ed. Vandenberg, E. J., Ed.; Plenum: New York, 1984; Vol. 5.
(13) Wunder, S. L.; S. D. Merajver, *J. Polym. Sci., Polym. Phys. Ed.*, in press.
(14) See, for example: de Gennes, P. G. *The Physics of Liquid Crystals*; Clarendon: Oxford, 1974. Kelker, H.; Hatz, R. *Handbook of Liquid Crystals*; Verlag Chemie: Weinheim, 1980; Chapter 3.
(15) Noel, C.; Laupretre, F.; Friedrich, C.; Fayolle, B.; Bosio, L. *Polymer* **1984**, *25*, 808.
(16) Matheson, R. R. *Macromolecules* **1980**, *13*, 643.
(17) Morgan, P. W. *Macromolecules* **1977**, *10*, 1381.
(18) Griffin, B. P.; Cox, M. K. *Br. Polym. J.* **1980**, *12*, 147.
(19) Luise, R. R., private communication.
(20) McFarlane, F. E.; Davis, T. G. (Eastman Kodak Co.) U.S. Patent 4 0111 199, 1977.
(21) Marrucci, G.; Ciferri, A. *J. Polym. Sci., Polym. Lett. Ed.* **1977**, *15*, 643.
(22) Kiss, G.; Porter, R. S. *J. Polym. Sci., Polym. Symp.* **1978**, *65*, 193.
(23) Alfonso, G. C.; Bianchi, E.; Ciferri, A.; Russo, S.; Salaris, F.; Valenti, B. *J. Polym. Sci., Polym. Symp.* **1978**, *65*, 213.